INTERNATIONAL JOURNAL FOR NUMERICAL METHODS IN ENGINEERING, VOL. 33, 1081–1105 (1992)

THE *s*-VERSION OF THE FINITE ELEMENT METHOD FOR MULTILAYER LAMINATES

J. FISH AND S. MARKOLEFAS

Rensselaer Polytechnic Institute, Troy, NY 12180, U.S.A.

SUMMARY

A methodology has been developed to accurately resolve the stress field in the vicinity of free edges as well as the overall response of laminated plates without significantly affecting the computational cost. This is accomplished by enriching a set of classical smooth interpolants throughout the thickness direction with C^0 continuous displacement interpolants (piecewise continuous strain field) in the regions where the most critical behaviour is anticipated. C^0 continuity of the displacement field is maintained by imposing homogeneous boundary conditions on the superimposed field in the portion of the boundary which is not contained within the boundary of the problem. Numerical experiments for both cylindrical bending and uniform extension of cross-ply laminates are presented to validate the present formulation.

1. INTRODUCTION

One of the major challenges in computational mechanics of composite materials is the development of advanced numerical techniques for resolving the structure of high gradients. Accurate resolution of the stress field in the vicinity of free edges is of great scientific interest and is necessary to predict various modes of failure in composite laminates. Theoretically, it is possible to capture the structure of the stress field by considering each layer as a three-dimensional monoclinic solid. Achenbach *et al.*[1] followed this approach by assuming linear distribution of displacements within each layer, while Spilker[2] used a mixed variational principle to enforce interlaminar traction continuity and free edge boundary conditions. However, if the stress field near free edges is to be accurately resolved in a composite plate made of more than 100 layers (not unusual in aircraft structures) with a uniform mesh of linear solid elements, a million-degrees-of-freedom mesh might be required. This number can be substantially reduced by the use of adaptive techniques (or by *a priori* employing fine mesh grading near free edges), but even so, such mesh refinement might be beyond the capacity of even the latest supercomputers.

A resolution of the computational complexity arising from three-dimensional modelling of individual layers has been attempted by various plate theories.[3–12] The classical laminated theory[3] and shear deformation plate theory[4] usually lead to reasonable predictions of the overall response (displacements, natural frequencies and buckling loads) but err badly in predicting interlaminar stresses. In general, the in-plane displacement field for various higher order plate theories can be expressed by

$$u_\alpha = \sum_{k=0}^{n} z^k u_{k\alpha}(x, y) \quad \alpha = 1, 2 \quad z \in (-t/2, t/2) \tag{1a}$$

0029–5981/92/071081–25$12.50
© 1992 by John Wiley & Sons, Ltd.

Received 31 August 1990
Revised 25 February 1991

and the transverse displacements

$$w = \sum_{k=0}^{m} z^k w_k(x, y) \quad z \in (-t/2, t/2) \tag{1b}$$

where t is the thickness of the plate. For example, $n = 1$ and $m = 2$ have been used by Whitney and Sun,[5] $n = m = 2$ by Nelson and Lorch,[6] and $n = 3$ and $m = 2$ by Lo *et al.*[7] More recently Levinson[8] and Reddy[9] used $n = 3$ and $m = 0$ and reduced the number of unknown parameters by, explicitly enforcing zero tractions on the bounding planes of the plate. Spilker and Jacobs[10] used $n = 1$ and $m = 0$ in the context of a mixed variational principle assuming linear variation of an assumed stress field.

Although these theories were extremely successful in predicting the overall response of structures, they were insufficient in estimating the stress fields in the vicinity of free edges. An attempt to improve the stress predictions by increasing the polynomial order of global interpolants (equations (1a) and (1b)) appears to be fruitless, since it leads to discontinuous tractions across the interfaces between the layers of different materials. By evaluating the coefficients of spectral series, it can be shown that the accuracy of spectral approximation depends mainly on the differentiability of the function being approximated, i.e., in the case of a C^0 continuous displacement function (discontinuous strain field) spectral approximation provides only second order accuracy, irrespective of the number of terms used in the spectral expansion. Furthermore, the use of higher order spectral interpolants significantly increases the condition number since the spectral interpolants are not orthogonal with respect to an inhomogeneous constitutive tensor, and thus the interlaminar stress predictions start to degrade as m and n become high.

An alternative approach to account for local effects by means of the boundary layer method that uncouples local calculations from overall analysis has been employed by several investigators.[11,13] By this technique it is possible to carry out classical laminated analysis, and to add, by linear superposition, a correcting stress field obtained separately by a boundary layer analysis. The correcting field is constructed so that free edge and interface conditions are satisfied exactly, and the asymptotic term decays rapidly with increasing distance from the free edge. However, the uncoupling into the two separate problems is effective only when the thickness is small compared to other dimensions (length and width).

The idea of locally enriching finite element solutions has been pioneered by Mote,[14] who introduced a 'global–local' formulation where 'global' shape functions were added to enrich the 'local' finite element field. By this technique, one can use special finite elements at the free edge with the nature of the fields prescribed *a priori*, while the unknown constants in the assumed field can be determined from the variational principle of the boundary value problem. This approach might be very useful if the nature of high gradients or the singularity is known *a priori*. However, as pointed out by Zwiers *et al.*,[15] the nature of the fields in multilayered laminates depends on the stacking sequence of the composite and the complete boundary conditions, and thus is problem dependent and needs to be determined for each case. An extensive review on various global–local methodologies can be found in Reference 16.

The objective of this work is to develop a general purpose robust computational tool to accurately resolve the stress field in the vicinity of free edges as well as the overall structural behaviour without significantly affecting the computational cost. This is achieved by combining a set of smooth global interpolants in $z \in (-t/2, t/2)$ (such as those given in equations (1a) and (1b)) with the C^0 displacement field defined locally within the layer. The additional field is superimposed only where high resolution of the stress field is required, usually where maximum interlaminar stress discontinuities occur, or as estimated by a posteriori error diagnosis. By this

technique accurate stress resolution will be obtained in critical regions, while elsewhere the resolution is sufficient only to predict the overall response with desired accuracy.

This work is an extension of the method recently reported by Fish,[17] to account for anisotropic and inhomogeneous media. It is specifically designed for a wide range of local problems in composite plates including free edge flexural and axial problems, plates with holes, joints, environmental and hygrothermal effects.

The idea of domain decomposition in laminated plates was originated by Pagano and Soni[18] who proposed to split the problem domain into two regions: the global domain where the smeared (effective) laminate properties are used and the local domain where each layer is interpolated separately. The stress continuity between the two regions and within the local region is enforced by means of the two-field variational principle. However, there are several important differences between this formulation and the present approach:

(i) In Reference 18, the boundary between the global and local domains is placed along the entire interface of connecting layers, while in the present work the location of the boundary can be arbitrary so that the local domain can be defined exactly where it is needed.

(ii) Probably the most significant difference between the two techniques is in computational efficiency and implementation. The major strength of the proposed method is in its *hierarchical* structure (linear problems), i.e., the stiffness matrix associated with the global interpolants is contained within the stiffness matrix of the refined model. This allows incorporation of the proposed computational model in the existing finite element codes with relative ease. Furthermore, the use of C^0 continuous higher order interpolants guarantees satisfaction of interface and free edge boundary conditions with desired accuracy which can be adjusted by controlling the local and global polynomial orders (obviously the singularity point is an exception). This eliminates the necessity for the mixed variational principle[18] and an accompanying cumbersome interface matching procedure.

The outline of this paper is as follows. Section 2 reviews the fundamental ideas of the finite element mesh superposition method and applies it to the laminated plates. Attention is restricted to two-dimensional problems. At this point no a posteriori error estimates at the global and local level have been incorporated into the computational model and the region of high gradients is assumed to be known *a priori*. Once the behaviour of the two-dimensional computational model is assessed, the method can be extended to three-dimensional plate-type problems with adaptive control of the optimal location of the local region and its discretization. Numerical results for both cylindrical bending and uniform extension of cross-ply laminates are given in Section 3.

2. FORMULATION

The basic idea of the *s*-version of the finite element method[17] is that a portion of the finite element mesh in which steep gradients are indicated by the solution is overlaid by a patch(s) of local meshes as shown in Figure 1. For the present application the problem domain Ω is assumed to be made up of a series of perfectly bonded layers stacked in the through-thickness (z) direction. The local regions where high gradients are anticipated can be encompassed by the domains Ω_L of arbitrary geometry, which are then subdivided into the element subdomains Ω_L^e. For the present application it is convenient to align the boundaries of the superimposed local domain along the co-ordinate axis, as shown in Figure 1. In the local regions, the displacement field $\mathbf{u}$ is approximated by superimposing the displacements resulting from the global finite element mesh $\mathbf{u}$ defined over the entire problem domain with the local field $\mathbf{u}^L$:

$$\mathbf{u} = \mathbf{u}^G + \mathbf{u}^L \quad \text{on } \Omega_L \tag{2a}$$

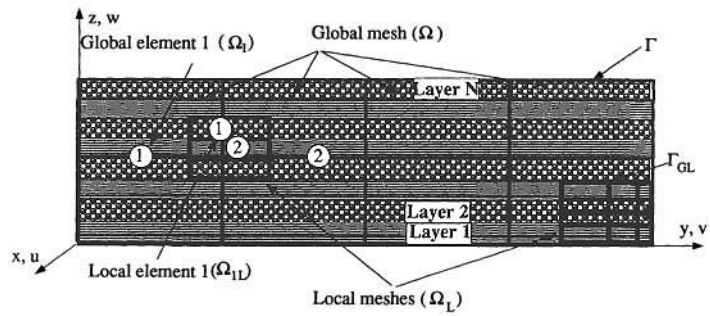

Figure 1. Typical example of the local and global meshes

where

$$\mathbf{u}^{\mathrm{L}} = \mathbf{0} \qquad \text{on } \Gamma_{\mathrm{GL}} \tag{2b}$$

and

$$\mathbf{u}^{\mathrm{G}} + \mathbf{u}^{\mathrm{L}} = \mathbf{u}^{\mathrm{p}} \qquad \text{on } \Gamma_u \tag{2c}$$

where Γ is the boundary of the problem domain Ω, which consists of the prescribed displacement boundary Γ_u and the prescribed traction boundary Γ_t. Γ_{GL} is the boundary between the two meshes.

Condition (2b) is required in order to satisfy C^0 continuity between the global and local finite element meshes. The inhomogeneous displacement boundary conditions $\mathbf{u}^{\mathrm{p}}$ can usually be taken care of by the global field $\mathbf{u}^{\mathrm{G}}$, although the accuracy of the prescribed displacement field can be significantly increased by subjecting the global field to $\mathbf{u}^{\mathrm{p}}$, and the remainder of the field, $(\mathbf{u}^{\mathrm{p}} - \mathbf{u}^{\mathrm{G}})$, can be accurately resolved by the superimposed mesh.

The global element displacement field can be constructed using the classical expressions given in equation (1), with m and n depending on the type of plate theory. However, it is computationally advantageous to define the displacement field in hierarchical fashion, so that, when element refinement is made, the element shape functions remain unchanged, and the polynomial order is increased by adding new terms. The two-dimensional hierarchical shape functions can be obtained by multiplication of one-dimensional hierarchical polynomials

$$u_k^G = N_{kA}(s, t)d_A \tag{3a}$$

$$N_{kA}(s, t) = H_J(s)H_I(t) \tag{3b}$$

where d_A are the global degrees-of-freedom; $s \in [-1, 1]$ and $t \in [-1, 1]$ are parametric coordinates in the y and z direction, respectively. The lower case subscripts indicate spatial components, while the upper case subscripts indicate degree-of-freedom. Standard tensorial notation is used with summation over the repeated indices. The set of one-dimensional hierarchical shape functions $H_I(r)$ is given by

$$H_1 = 1/2\,(1 - r) \tag{4a}$$

$$H_2 = 1/2\,(1 + r) \tag{4b}$$

$$H_{K+2} = \int_{-1}^{r} P_K(\xi)\,\mathrm{d}\xi \quad K = 1, 2, \ldots \tag{4c}$$

where r is a parametric co-ordinate $r \in [-1, 1]$ and $P_K(\xi)$ is a Legendre polynomial of degree K defined by

$$P_K(\xi) = \frac{1}{(K-1)!}\frac{1}{2^{K-1}}\frac{\mathrm{d}^K}{\mathrm{d}\xi^K}[(\xi^2 - 1)^K] \tag{5}$$

The resulting two-dimensional shape functions (3b) and corresponding degrees-of-freedom are termed as nodal ($I, J \leqslant 2$), side ($I \leqslant 2, J > 2$ and $J \leqslant 2, I > 2$) and internal ($I, J > 2$). For a detailed discussion on hierarchical elements, see Peano[19] and Zienkiewicz and Morgan.[20]

The polynomial order of the global field will mainly depend on the desired accuracy of the global response (displacements, natural frequencies, buckling loads, etc.) However, the stress gradients in laminate composites cannot be efficiently resolved by increasing the polyomial order of smooth interpolants alone, and thus additional displacement interpolants with discontinuous first derivatives (C^0 continuity) are needed to capture the local behaviour efficiently. The local or superimposed field is composed of C^0 continuous elements with element boundaries aligned along the interfaces of the layers. Some general guidelines on designing local meshes are provided in Section 3, although the issue of finding the optimal location of the superimposed field and its discretization is not addressed here and will be presented elsewhere.

The interpolants on local elements, similarly to the global ones, will be cast into the hierarchical form

$$u_k^{\mathrm{L}} = N_{kA}^{\mathrm{L}}(s, t)a_A \tag{6a}$$

$$N_{kA}^{\mathrm{L}}(s, t) = H_J(s)H_I(t) \tag{6b}$$

where N_{kA}^{L} and a_A are local shape functions and their respective degrees-of-freedom.

C^0 continuity condition (2b), or a compatibility between the two meshes, is imposed by constraining the nodal and side degrees-of-freedom on the boundary between the meshes

$$a_A|_{\Gamma_{\mathrm{GL}}} = 0 \tag{7}$$

Discrete equilibrium equations can be obtained from the principle of virtual work, which states

$$\int_\Omega \delta u_{(i,j)} D_{ijkl} u_{(k,l)}\,\mathrm{d}\Omega - \int_{\Gamma_t} \delta u_i t_i\,\mathrm{d}\Gamma - \int_\Omega \delta u_i b_i\,\mathrm{d}\Omega = 0 \quad \forall\,\delta\mathbf{u} \tag{8}$$

where D_{ijkl} is a piecewise continuous constitutive tensor of the laminate, b_i and t_i are the body forces and prescribed tractions, respectively, and the prefix δ designates a variation.

The displacement test function $\delta\mathbf{u}$, similarly to the trial function, is given by the superposition of the test function in the two fields:

$$\delta\mathbf{u} = \delta\mathbf{u}^{\mathrm{G}} + \delta\mathbf{u}^{\mathrm{L}} \tag{9}$$

where the displacement test function is required to be C^0 and vanish on Γ_u, so

$$\delta\mathbf{u}^{\mathrm{G}} = \delta\mathbf{u}^{\mathrm{L}} = 0 \quad \text{on } \Gamma_u \tag{10}$$

Discrete equations are obtained by substituting interpolants (3)–(6) into (8) and requiring arbitrariness of local and global variations. The basic structure of the resulting equations is summarized below:

$$\begin{pmatrix} K_{\mathrm{AD}}^{\mathrm{G}} & K_{\mathrm{AE}}^{\mathrm{C}} \\ K_{\mathrm{BD}}^{\mathrm{C}} & K_{\mathrm{BE}}^{\mathrm{L}} \end{pmatrix} \begin{pmatrix} d_{\mathrm{D}} \\ a_{\mathrm{E}} \end{pmatrix} = \begin{pmatrix} f_{\mathrm{A}}^{\mathrm{ext}} \\ h_{\mathrm{B}}^{\mathrm{ext}} \end{pmatrix} \tag{11}$$

$$K_{\mathrm{AD}}^{\mathrm{G}} = \int_\Omega N_{(i\mathrm{A},j)} D_{ijkl} N_{(k\mathrm{D},l)}\,\mathrm{d}\Omega \tag{12a}$$

$$K^{L}_{BE} = \int_{\Omega_L} N^{L}_{(iB,j)} D_{ijkl} N^{L}_{(kE,l)} \, d\Omega \tag{12b}$$

$$K^{C}_{AE} = \int_{\Omega_L} N_{(iA,j)} D_{ijkl} N^{L}_{(kE,l)} \, d\Omega \tag{12c}$$

$$f^{ext}_{A} = \int_{\Gamma_t} N_{iA} t_i \, d\Gamma + \int_{\Omega} N_{iA} b_i \, d\Omega \tag{12d}$$

$$h^{ext}_{B} = \int_{\Gamma_t} N^{L}_{iB} t_i \, d\Gamma + \int_{\Omega_L} N^{L}_{iB} b_i \, d\Omega \tag{12e}$$

Remark 1

Immediately we observe the hierarchical structure of the stiffness matrix: the global stiffness matrix $\mathbf{K}^G$ is contained (for linear problems) within the total stiffness of the refined grid. For example, if global interpolants were of the form given in equation (1) with $n = 1$ and $m = 0$, $\mathbf{K}^G$ would correspond to the stiffness matrix obtained from the shear deformation plate theory, and thus the implementation of the present technique will result in hierarchical augmentation of the global stiffness matrix by the local ($\mathbf{K}^L$) and the coupling ($\mathbf{K}^C$) stiffness terms as shown in equation (11).

Remark 2

At first glance, the proposed method may appear to be quite similar to and of no advantage over the classical substructuring techniques. However, the uniqueness of the *s*-method (and also the recently published spectral overlay method[21]) is that a precise location of regions that require a more detailed interrogation does not need to be known *a priori* to performing global analysis. Such regions may be obvious, such as cutouts, sharp corners, joints, or not so obvious, such as a locally buckled panel loaded in compression, force dependent high gradient fields, or some failure propagation processes, such as crack propagation, shear banding and fibre microbuckling. Thus if a substructuring method is to be employed, additional global analysis is needed once the precise location of the critical regions is identified.

Remark 3

The constitutive tensor in composite laminates is a piecewise continuous function throughout the thickness, and therefore, the exact evaluation of the stiffness matrix (either numerical or analytical) requires that the integration throughout the thickness will be separately performed within each layer.

Remark 4

Special care must be exercised to avoid the singularity of the tangent stiffness matrix. The singularity or rank deficiency occurs if the superimposed and underlying meshes have identical deformation modes. The two meshes will have the same modes if there is a patch of elements in the local mesh having entire boundaries aligned along the element sides in the global mesh. The redundant degrees-of-freedom can be constrained by eliminating equations with zero pivots which are encountered in the course of the factorization process.

3. NUMERICAL EXAMPLES

Two problems representing both singular and non-singular solutions have been numerically analysed to demonstrate and validate the present formulation. In the first example (non-singular solution), we consider a cylindrical bending of a symmetric cross-ply laminate with various numbers of layers and thickness–span ratios subjected to a transverse sinusoidal loading, while in the second example (singular solution), we analyse a four-layer symmetric cross-ply laminate subjected to a prescribed uniform in-plane normal strain. Geometry, boundary and symmetry conditions, layup configuration and material properties for both problems are shown in Figure 2.

For the cylindrical bending problem three cases are considered:

Case 1: $2L/b = 4$; Layup = (90/0/90)

Case 2: $2L/b = 8$; Layup = (90/0/90)

Case 3: $2L/b = 8$; Layup = $(90/0)_6$ starting from the bottom layer

where b and $2L$ are the thickness and the width of the laminate; fibre orientation is measured with respect to the x axis as shown in Figure 2.

For the axial tension problem, a single case of the symmetric cross-ply laminate with $(0/90)_s$ layup construction and 0·25 thickness–width ratio has been considered. Under uniform extension of a cross-ply laminate, the displacement field is assumed to be of the form

$$u_x = u(x) = x\bar{\varepsilon}_x \qquad u_y = v(y, z) \qquad u_z = w(y, z) \tag{13}$$

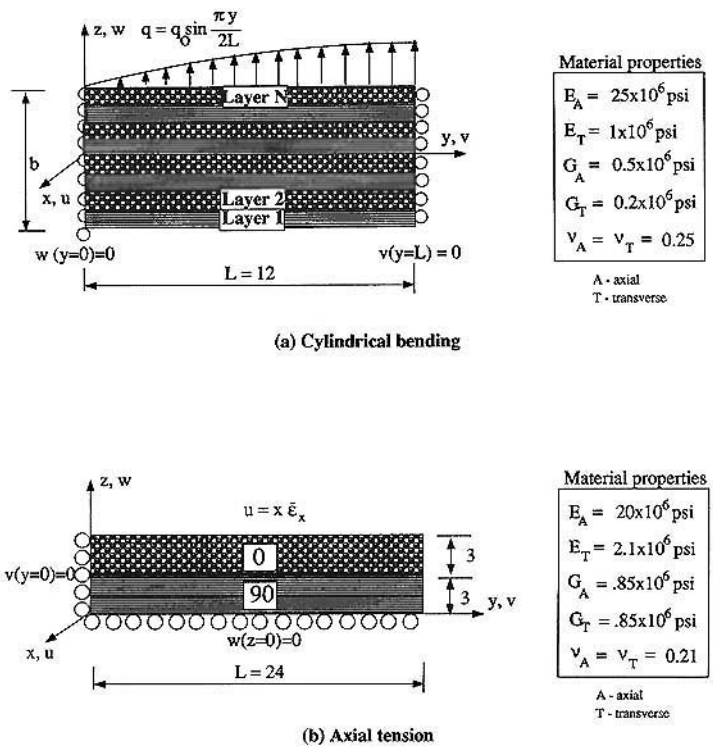

Figure 2. Geometry and material properties for the test cases

For the purpose of comparison we will test three formulations, which are called:

Global p-version: A higher order plate theory where a single element is used throughout the thickness. Identical polynomial order pg is used to interpolate both v and w.

Layerwise p-version: Solid, or plane-strain in 2D, modelling of each layer. Identical polynomial order p is used to interpolate both v and w.

s-version: Present superposition method. Uniform polynomial order pg is used for the global mesh and polynomial order s is used for the local mesh.

Numerical results for the cylindrical bending problem (Cases 1, 2) are compared to the elasticity solution given by Pagano,[22] while for the twelve-layer problem (Case 3), results are compared with those obtained using a fine mesh of higher order elements. Numerical results for the axial tension problem are compared with those obtained by Wang and Crossman[23] and Spilker.[24]

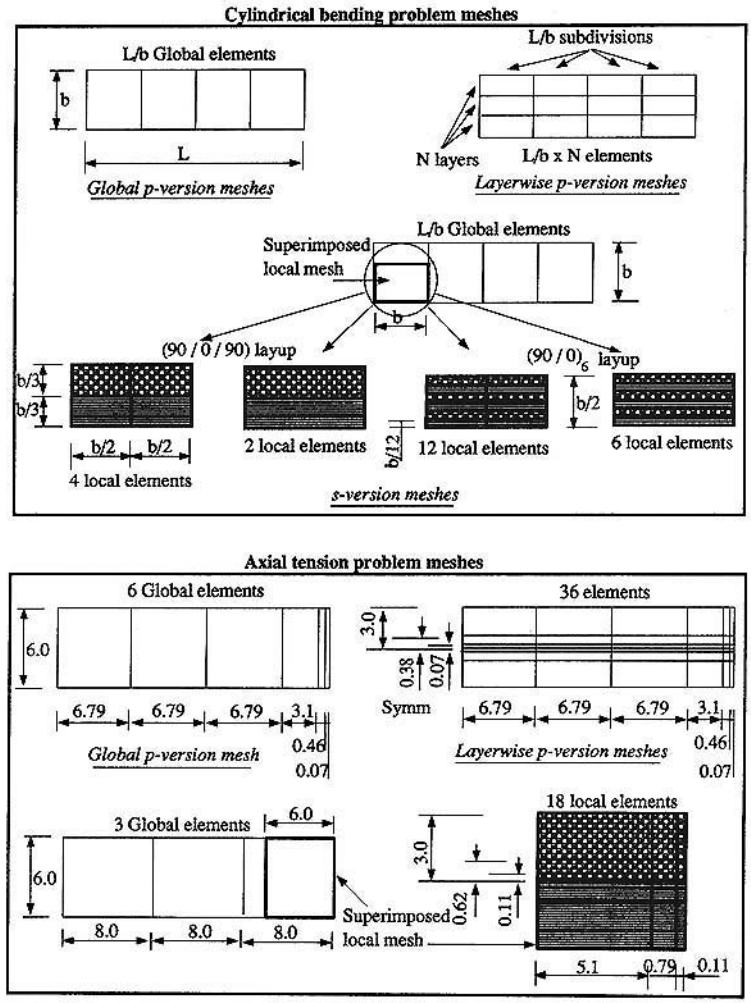

Figure 3. The finite element models for the test cases

The finite element meshes for all test problems are presented in Figure 3. The issue of finding the optimal location of the superimposed field, its subdivision, and the polynomial order of the superimposed elements is not addressed here. Instead, some experience gained with p-[25] and s-methods[17] is used here as a general guideline to construct the superimposed meshes. For the cylindrical bending problem (non-singular solution) a minimal number of elements aligned along the layer interfaces is used to construct the local mesh. For problems with singularities, such as in the case of axial tension, the local meshes are strongly graded towards the singularity, with the element size reduced in geometric progression by a factor of about 0·15. For all test problems considered here, the local mesh extended the distance equal to the thickness of the laminate from

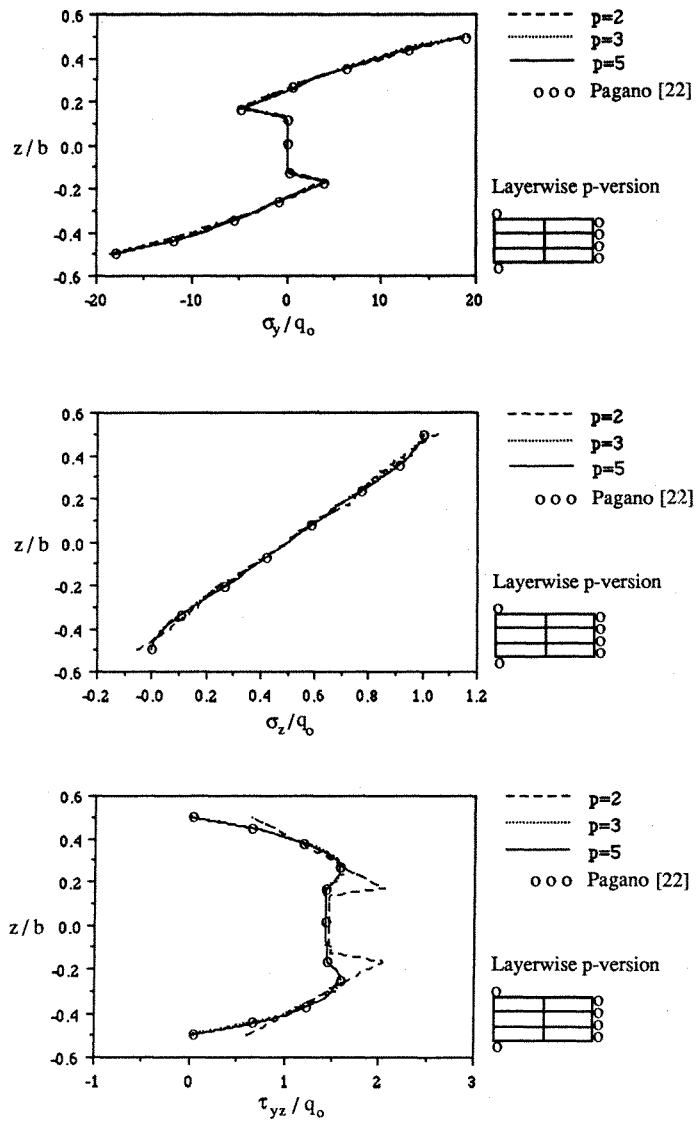

Figure 4. Stress distribution across the midspan in the 90/0/90 laminate and $2L/b = 4$ subjected to sinusoidal loading in cylindrical bending as obtained with the layerwise p-version of the finite element method

the free edge—the region where the most critical behaviour (high interlaminar stress gradients) is anticipated.

Figure 4 shows the normalized stress distributions $(\sigma_y, \sigma_z)/q_0$ at the midspan and τ_{yz}/q_0 at $y = 0$ throughout the thickness for the three-layer problem and $2L/b = 4$ (Case 1) as obtained with the layerwise p-method for increasing polynomial orders. It is observed that the σ_y and σ_z distributions for polynomial orders ranging from 2 to 5 are in good agreement with the elasticity solution; however, the shear stress for $p = 2$ is discontinuous across the layer interfaces and exhibits 30 per cent difference in the maximum stress value, while for $p = 3$ the results converge to the elasticity solution with less than 1 per cent difference.

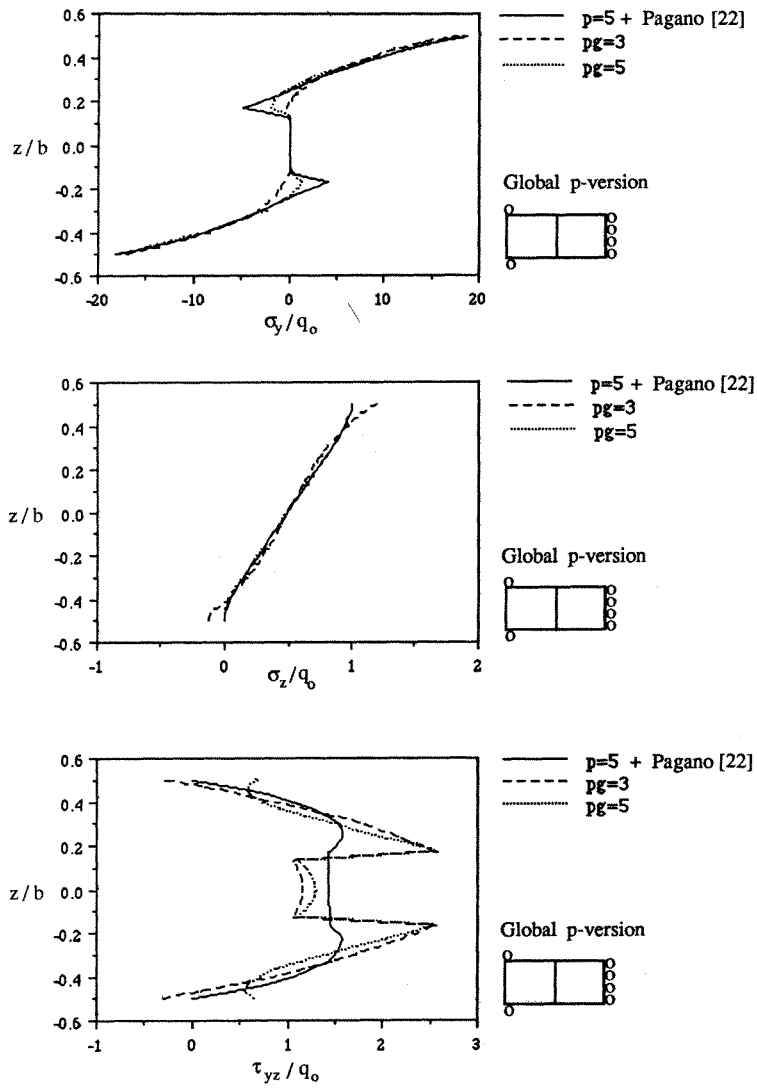

Figure 5. Stress distribution across the midspan in the 90/0/90 laminate and $2L/b = 4$ subjected to sinusoidal loading in cylindrical bending as obtained with the global p-version of the finite element method

The global *p*-version (higher order multilayer plate) solution for the case study 1 is shown in Figure 5 for global polynomial orders 3 and 5. The results show that increasing global polynomial order from 3 to 5 only slightly improves the axial stress predictions but has no significant effect on the transverse shear distribution, rendering the discrepancies at the interfaces and at the stress-free boundaries.

Numerical results for the *s*-version of the finite element method with global polynomial order $pg = 5$ and the local polynomial order $s = 5$ are shown in Figure 6. It can be seen that the normal stress distribution is in excellent agreement with the elasticity solution, while differences in the

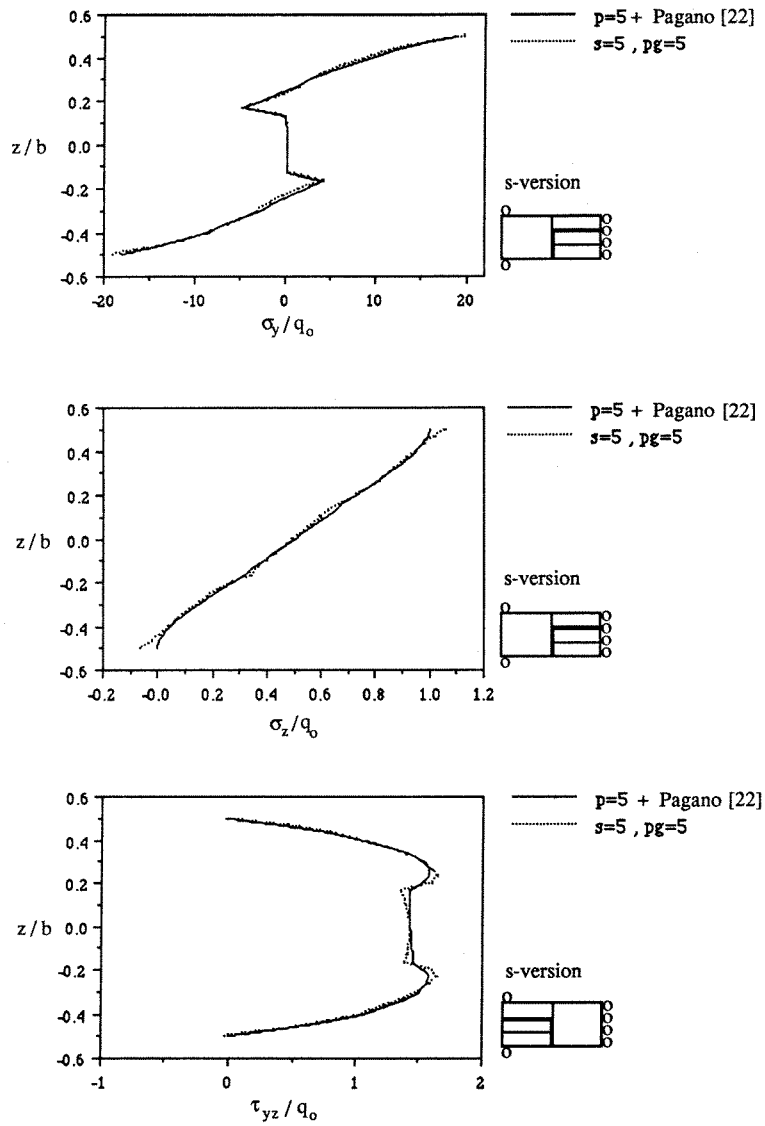

Figure 6. Stress distribution across the midspan in the 90/0/90 laminate and $2L/b = 4$ subjected to sinusoidal loading in cylindrical bending as obtained with the *s*-version of the finite element method

shear stress at the layer interface are less than 6 per cent. These slight differences are attributed to the fact that the boundary between the local and global meshes Γ_{GL}, acting as a source of disturbance on the stress field, is very close to the local domain of interest. The results can be further improved by pushing Γ_{GL} away from the local domain of interest.

The results for the moderately thin laminate ($2L/b = 8$) with the same layup construction (Case 2) show a similar trend (see Figures 7, 8 and 9): the layerwise p-method with $p = 3$ matches well the elasticity solution for all the stress components; the global p-version exhibits severe discon-

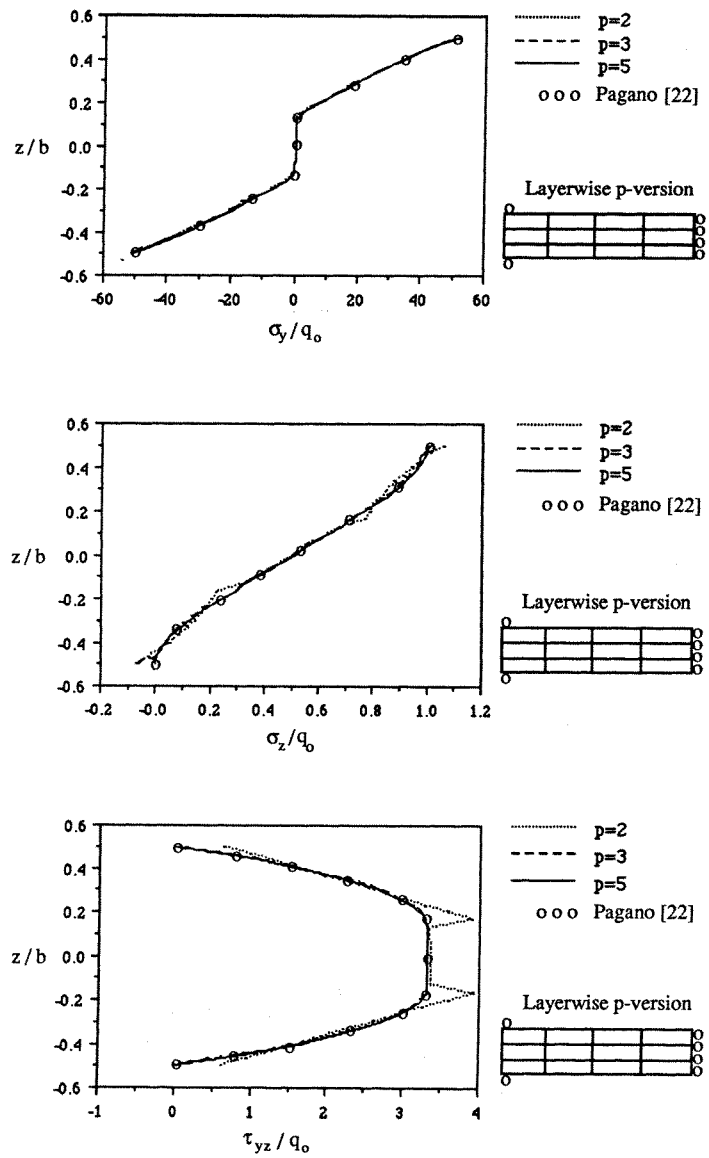

Figure 7. Stress distribution across the midspan in the 90/0/90 laminate and $2L/b = 8$ subjected to sinusoidal loading in cylindrical bending as obtained with the layerwise p-version of the finite element method

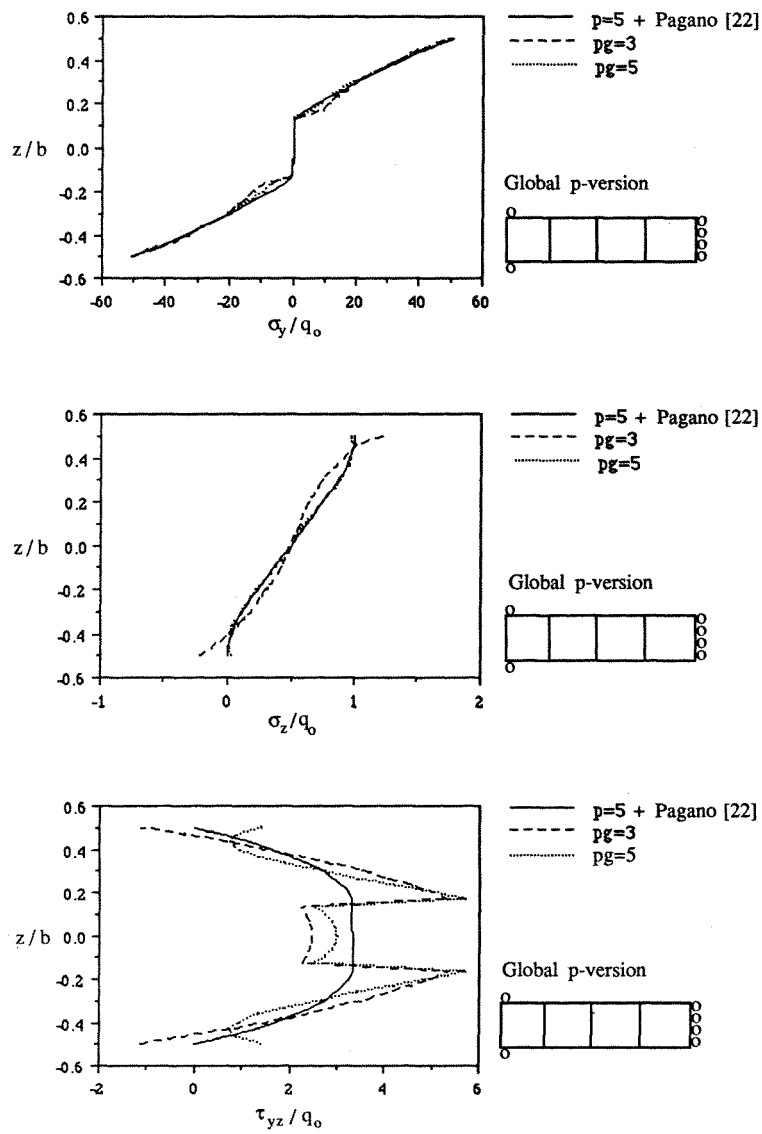

Figure 8. Stress distribution across the midspan in the 90/0/90 laminate and $2L/b = 8$ subjected to sinusoidal loading in cylindrical bending as obtained with the global p-method

tinuities at interfaces and significantly violates the stress-free boundary conditions irrespective of the global polynomial order; the s-version provides an excellent result for the normal stress and exhibits differences which do not exceed 6 per cent for the shear stresses. Note that for the problem with only three layers there is no significant computational advantage gained by using the s-method as opposed to the layerwise p-version. The computational advantage becomes significant with increasing the number of layers, as will be shown in our next numerical example.

Figure 10 shows the normalized stress distribution throughout the thickness at the midspan for the 12-layer problem and thickness/span ratio equal to 8 (Case 3) as obtained using the layerwise

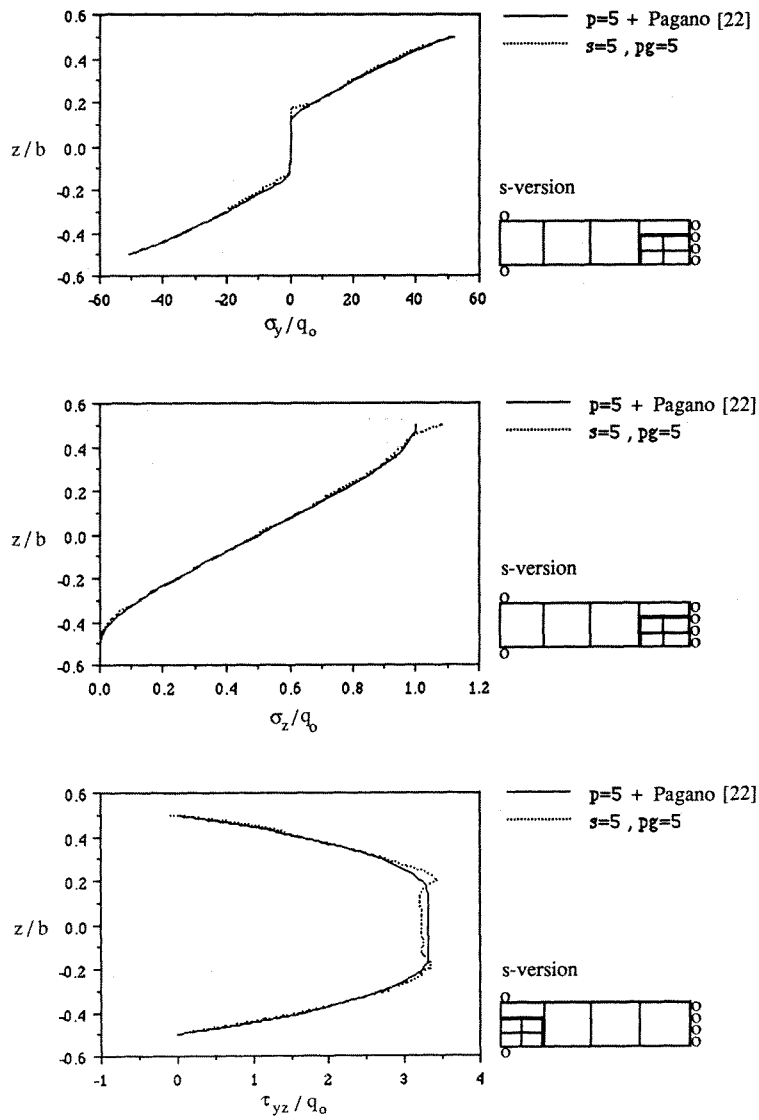

Figure 9. Stress distribution across the midspan in the 90/0/90 laminate and $2L/b = 8$ subjected to sinusoidal loading in cylindrical bending as obtained with the *s*-method

p-method. The results indicate differences of less than 1 per cent between the solutions obtained with polynomial orders 3 and 5. Furthermore, unlike in the previous case, the stresses are reasonably good for $p = 2$, showing an error of less than 2 per cent in σ_y and σ_z, and 6 per cent in τ_{yz}. The layerwise *p*-version finite element model shown in Figure 3 consists of 1192, 504 and 304 degrees-of-freedom (d.o.f.) for the polynomial orders of 5, 3 and 2 respectively.

The number of degrees-of-freedom in the global *p*-version finite element model is significantly smaller: 136 d.o.f. for $pg = 5$ and 64 d.o.f. for $pg = 3$. Although axial stress predictions as shown in Figure 11 are in a good agreement with the elasticity solution in the case of the axial stress, the interlaminar stress components show severe oscillations.

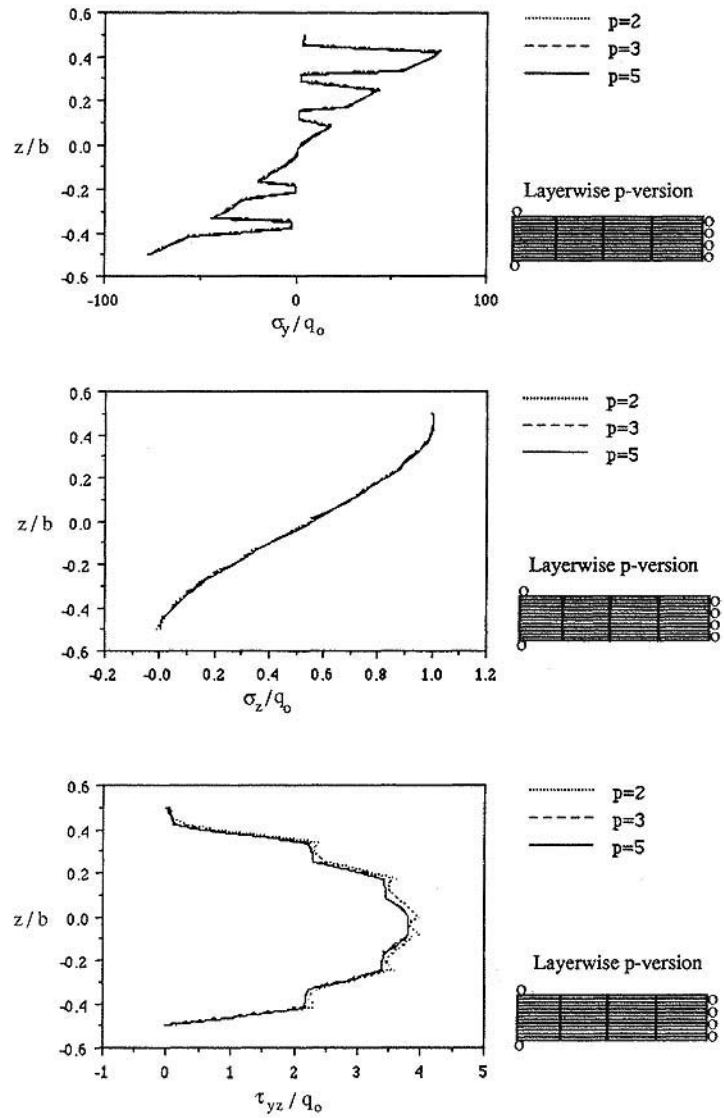

Figure 10. Stress distribution across the midspan in the $(90/0)_6$ laminate and $2L/b = 8$ subjected to sinusoidal loading in cylindrical bending as obtained with the layerwise p-method

The s-version finite element model examined here consists of either 12- or 6-local-element-meshes superimposed at the bottom half of the first global element, as shown in Figure 3. The objective of this example is to show the ability of the proposed technique to accurately resolve the stress distribution in local regions. Stress distributions for the 12-local-element case with global and local polynomial orders equal to 3 (total of 152 d.o.f.) are shown in Figure 12. These results reveal comparable quality of the solution in the local region to the one obtained with the layerwise p-version using $p = 2$, but at the expense of 50 per cent reduction in the number of degrees-of-freedom. Computational savings will become even more dramatic as the number of layers is increased.

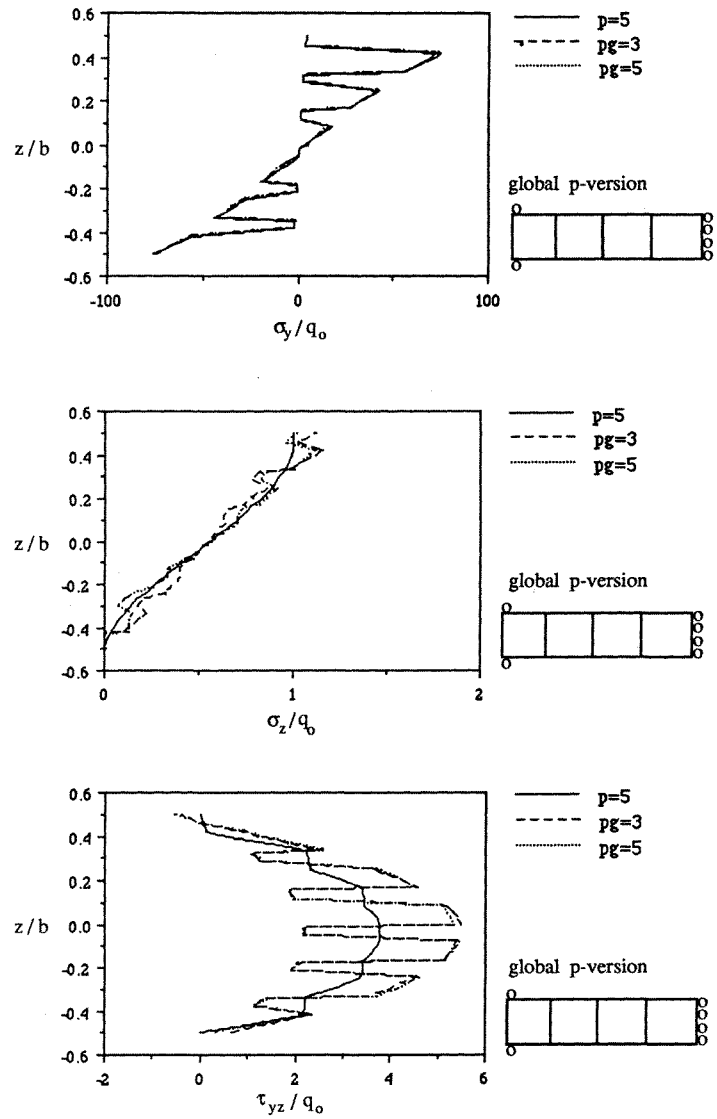

Figure 11. Stress distribution across the midspan in the $(90/0)_6$ laminate and $2L/b = 8$ subjected to sinusoidal loading in cylindrical bending as obtained with the global p-method

Somewhat surprising results are presented in Figure 13. Figure 13(a) shows that reducing the global polynomial order from 3 to 2 significantly degrades the shear stress predictions, and even increasing the local polynomial order from 3 to 5 does not improve the results. Figure 13(b) shows that reducing the number of elements and increasing both global and local polynomial orders does not increase the rate of convergence as one would expect in the case of smooth solutions. As an example, a 6-local-element mesh with $pg = s = 5$, which has a comparable quality of the solution to the one obtained with 12-local-element mesh and $pg = s = 3$, has almost 70 per cent more degrees-of-freedom.

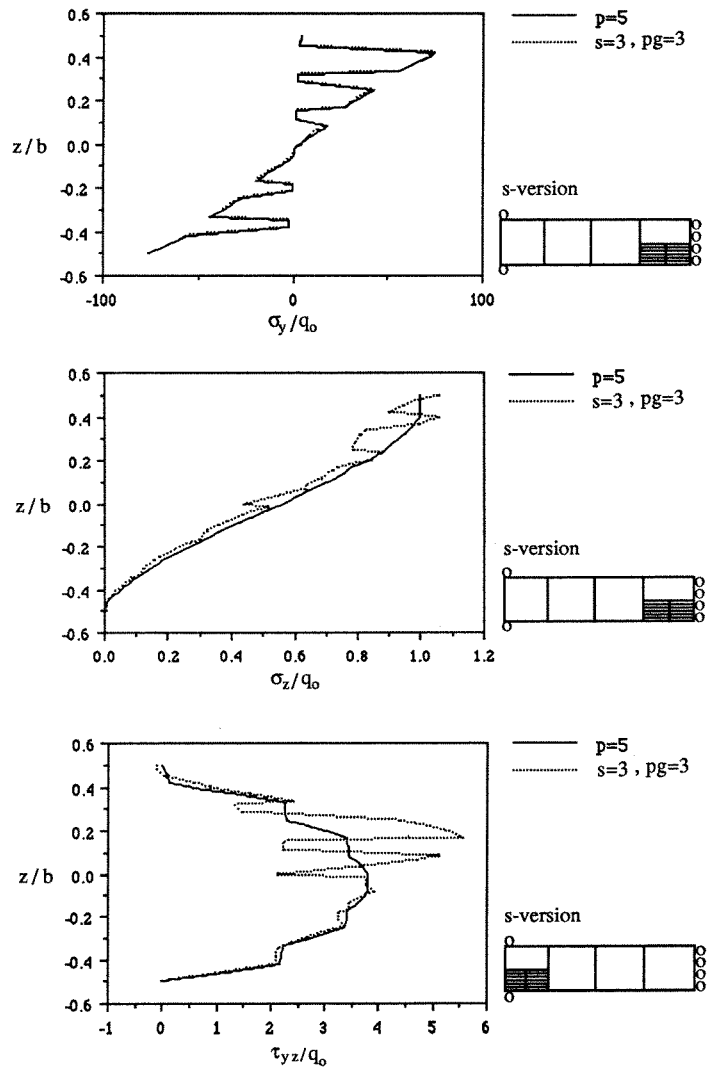

Figure 12. Stress distribution across the midspan in the $(90/0)_6$ laminate and $2L/b = 8$ subjected to sinusoidal loading in cylindrical bending as obtained with the *s*-method

Next we proceed with the axial tension problem (see Figure 2 for geometry and material properties, and Figure 3 for finite element meshes). Figure 14 shows the contour plots (14(a)) and the distribution of σ_z along $z = 0$ (14(c)) and $z = h \pm \varepsilon$, $\varepsilon \to 0$ (14(b)) as obtained with the layerwise *p*-version using $p = 5$. Figure 15 presents the contour plots and a shear stress distribution along the interface. It is observed that for $y/b < 0{\cdot}993$ both σ_z and τ_{yz} are continuous across the interface of the 90/0 layers (less than 0·5 per cent differences), and only at the singularity point there is a significant discontinuity of the peeling and shear stresses. Furthermore, it can be seen from the contour plots that the free edge boundary conditions are accurately satisfied except for the immediate vicinity of the singularity point.

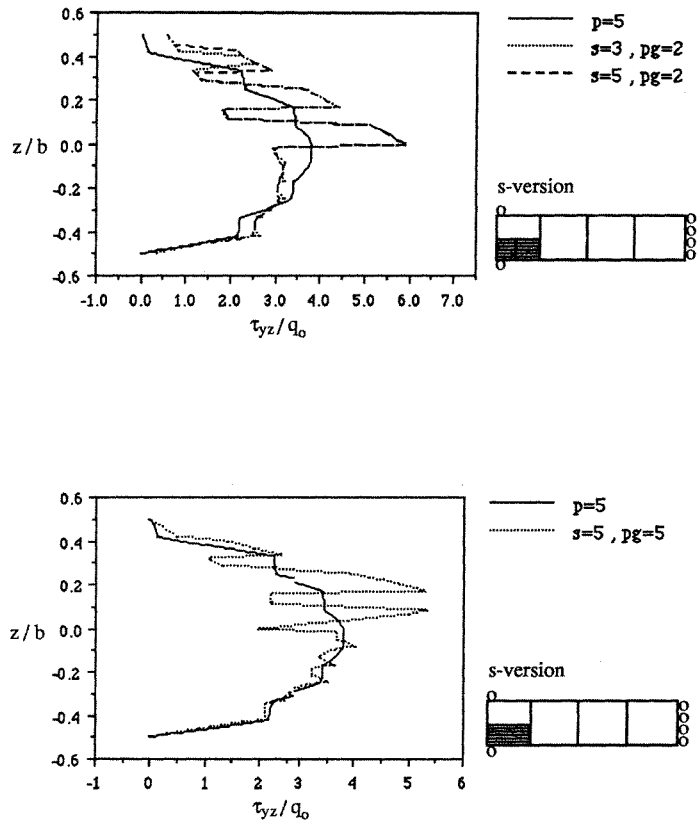

Figure 13. Examples of the local mesh design

Contour plots, peeling and shear stress distributions at the interface ($z = h$) computed with the global p-version using $pg = 5$ are shown in Figures 16 and 17. It can be seen that the free edge boundary conditions are generally violated and significant peeling stress discontinuities are encountered across the interface at $z = h$. Since the shear modulus is assumed to be homogeneous and isotropic, the resulting shear stress is absolutely continuous along $z = h$ and vanishes at the free edge, showing a good agreement with Reference 24 along this line.

Numerical results of the axial tension problem obtained with the s-version of the finite element method using $pg = s = 5$ are shown in Figures 18, 19. It is observed that ther stress distributions in the local region are almost identical to those obtained using the layerwise p-method (but at much lower expense) and are in good agreement with those from References 23 and 24. It can be seen that at the boundary between the two meshes ($y = 18$) there is a discontinuity in the shear stress. This is attributed to the fact that only C^0 continuity is imposed between the meshes and hence the stress field might be discontinuous there.

4. SUMMARY AND FUTURE RESEARCH DIRECTIONS

A methodology has been developed to enhance the finite element computations in multilayered laminates. The method consists of overlaying a global finite element mesh with a local mesh in the

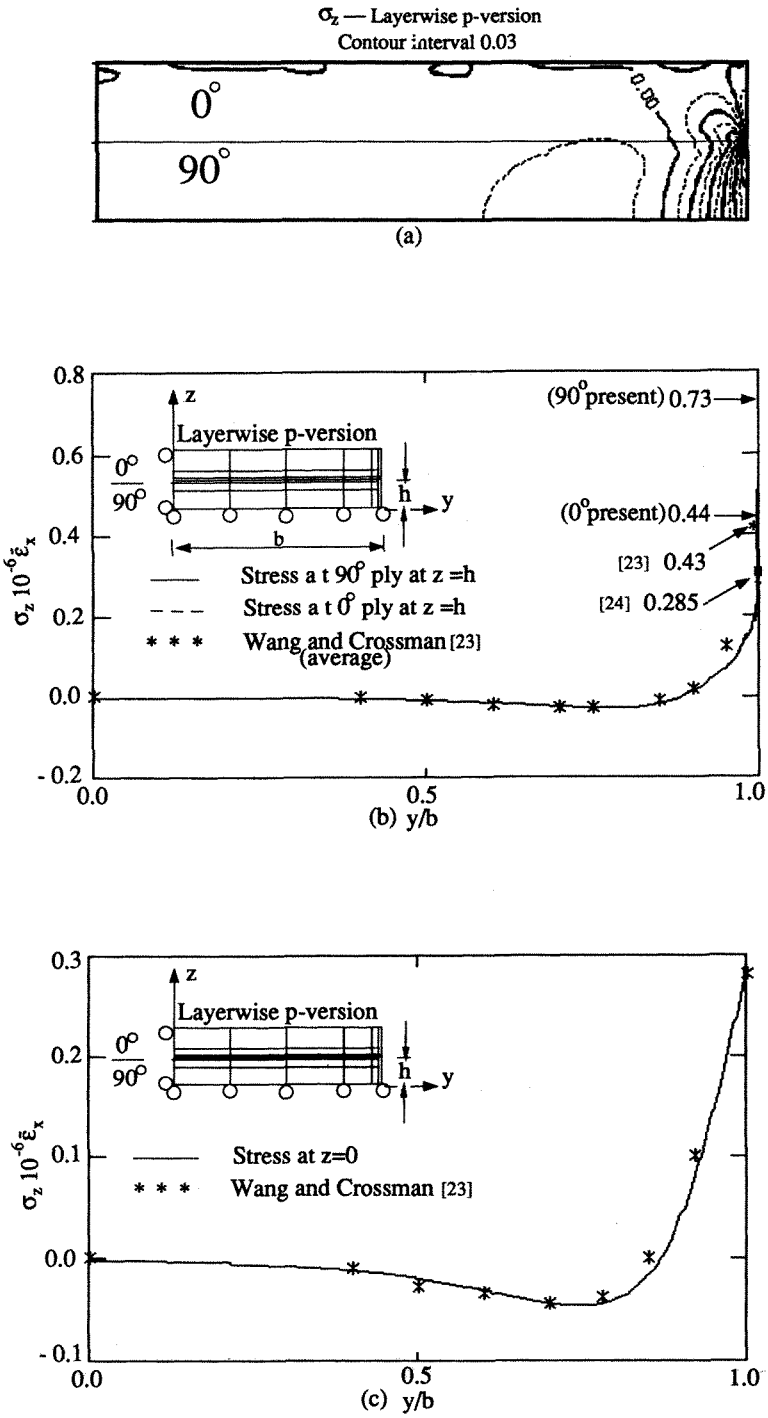

Figure 14. Contour plots and distribution of σ_z along $z = 0$ and $z = h$ in axial tension problem as obtained with layerwise p-method

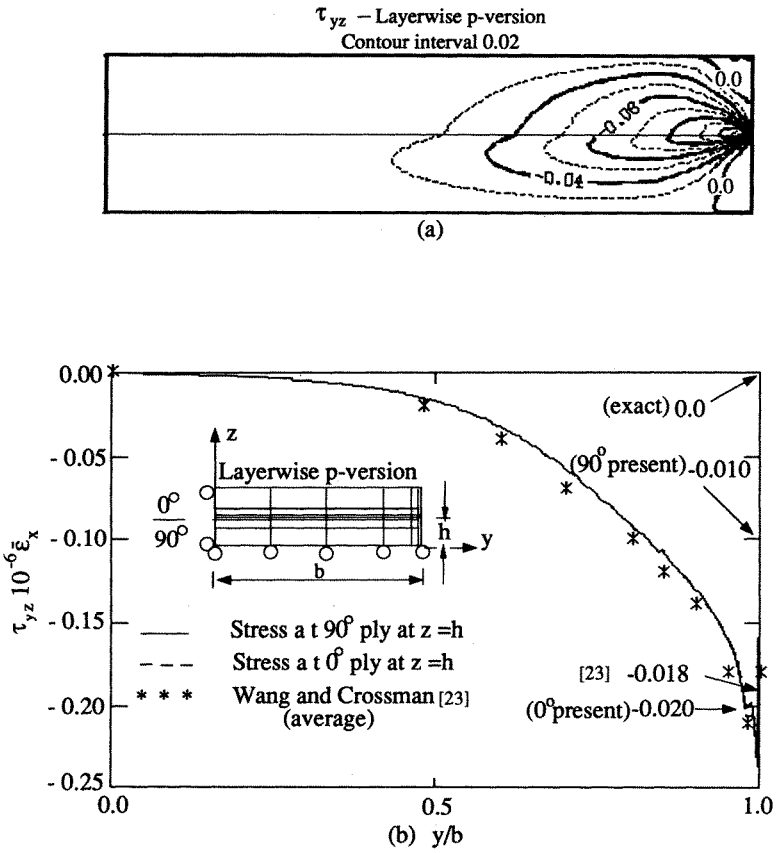

Figure 15. Contour plots and distribution of τ_{yz} along $z = h$ in axial tension problem as obtained with layerwise p-method

regions where high gradients are indicated by the solution. Unlike the boundary layer method where the solution is split into separate global and local problems, the present method is able to take a full account of the coupling phenomenon between the global and local response, which appears to be of major influence on interlaminar stress distribution. The 12-layer-local-element mesh cylindrical bending example confirms this finding: reduction in a global polynomial order had a drastic effect on the shear stress distribution in the vicinity of the free edge which could not be significantly improved by increasing a local polynomial order. The issue of optimal balance between the two meshes, the optimal placement of the local regions and its discretization is not addressed here and is one of the topics of our future research.

Much greater computational savings are expected if the present formulation is extended to accommodate general three-dimensional multilayer laminates. In such an extension a solid modelling of individual layers may not be feasible and the importance of isolating the region of critical behaviour by means of a posteriori error analysis would be of great importance. Within the framework of hierarchical shell modelling[26], a layerwise solid model can be superimposed on

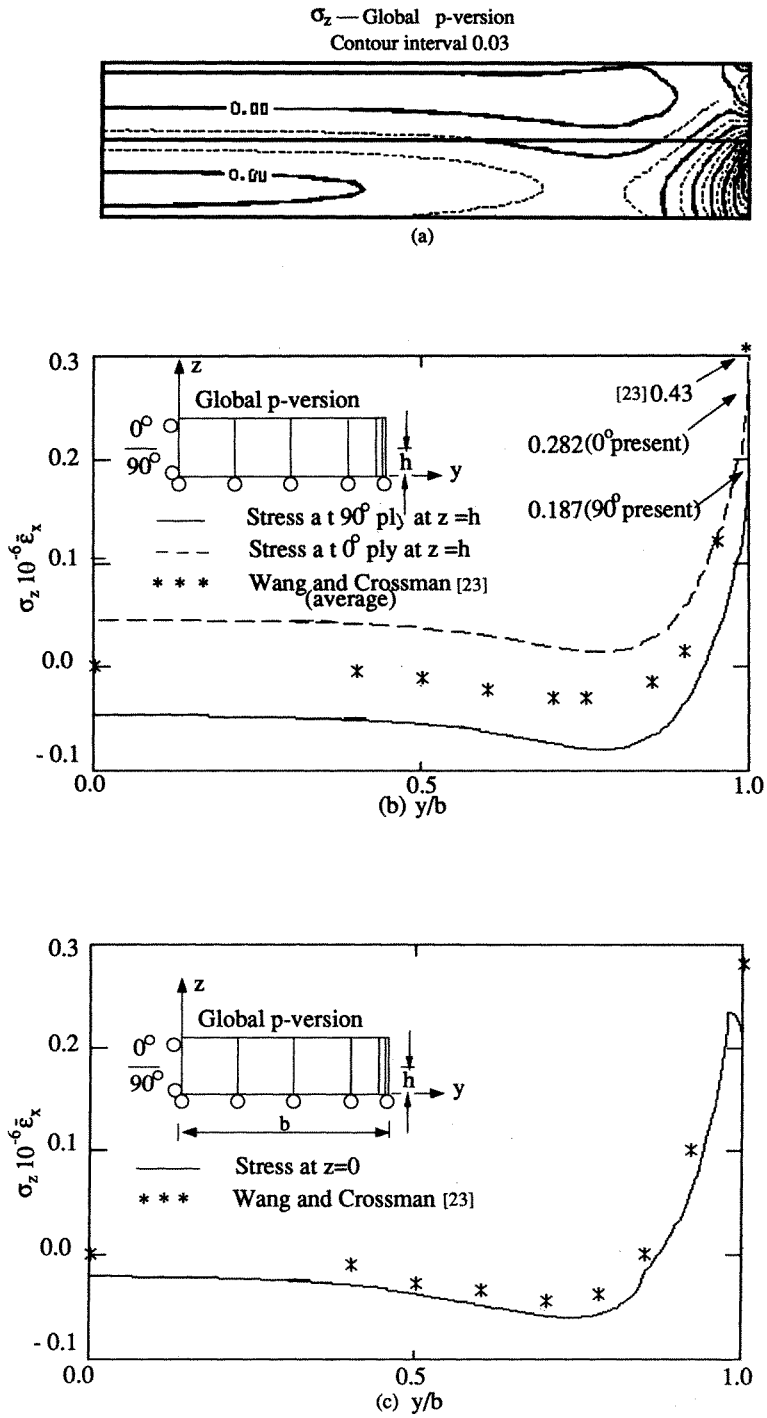

Figure 16. Contour plots and distribution of σ_z along $z = 0$ and $z = h$ in axial tension problem as obtained with global p-method

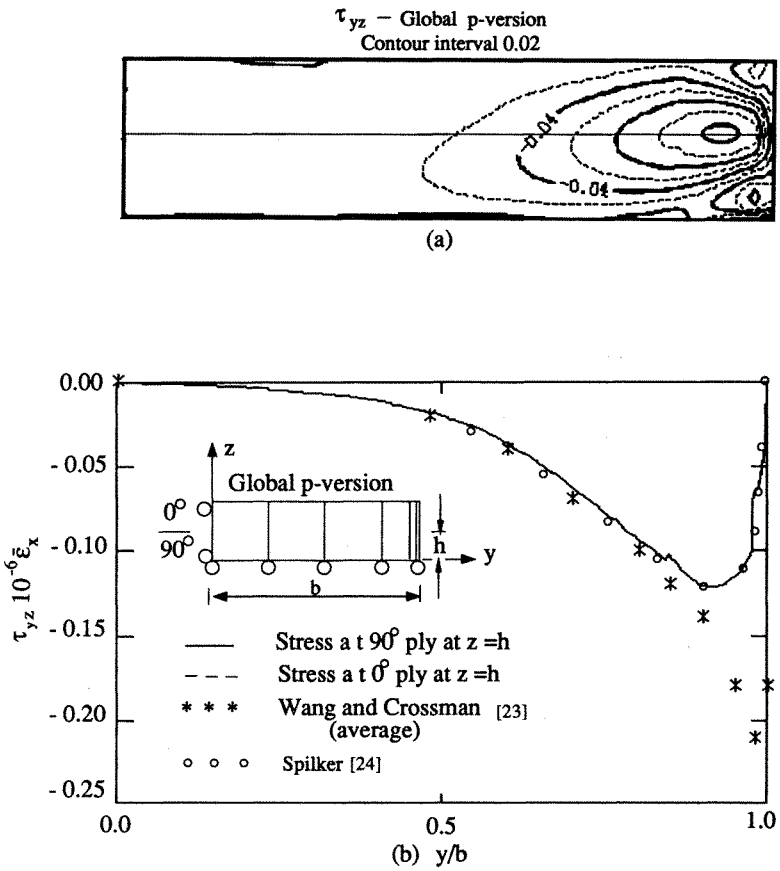

Figure 17. Contour plots and distribution of τ_{yz} along $z = h$ in axial tension problem as obtained with global p-method

the shell model in the critical regions. Displacement continuity can be enforced by constraining *nodal*, *edge* and *face* modes on the boundary between the two domains. If desired, the hierarchical degrees-of-freedom can be correlated to the midplane displacements, rotations and higher order generalized degrees-of-freedom employing similar procedures reported by Reddy,[9] and consequently, the stiffness matrix in terms of conventional degrees-of-freedom can be constructed.

In real multilayered laminates, every layer is heterogeneous and thus high gradients can occur at the interfaces between fibres and matrix, and not only at a layer interface. The distance over which the interface singularities extend their influence is of the order of magnitude of several fibre diameters, rendering our basic assumption of piecewise continuous constitutive tensor questionable. The method presented here is, in fact, a multiscale computational technique which can be successfully applied to model phenomena at several different scales. This can be accomplished by superimposing an additional mesh, say micro-mesh, on top of the local mesh in the regions where micro behaviour is being investigated. Such studies could be again carried out in two dimensions prior to extension to the general three-dimensional case.

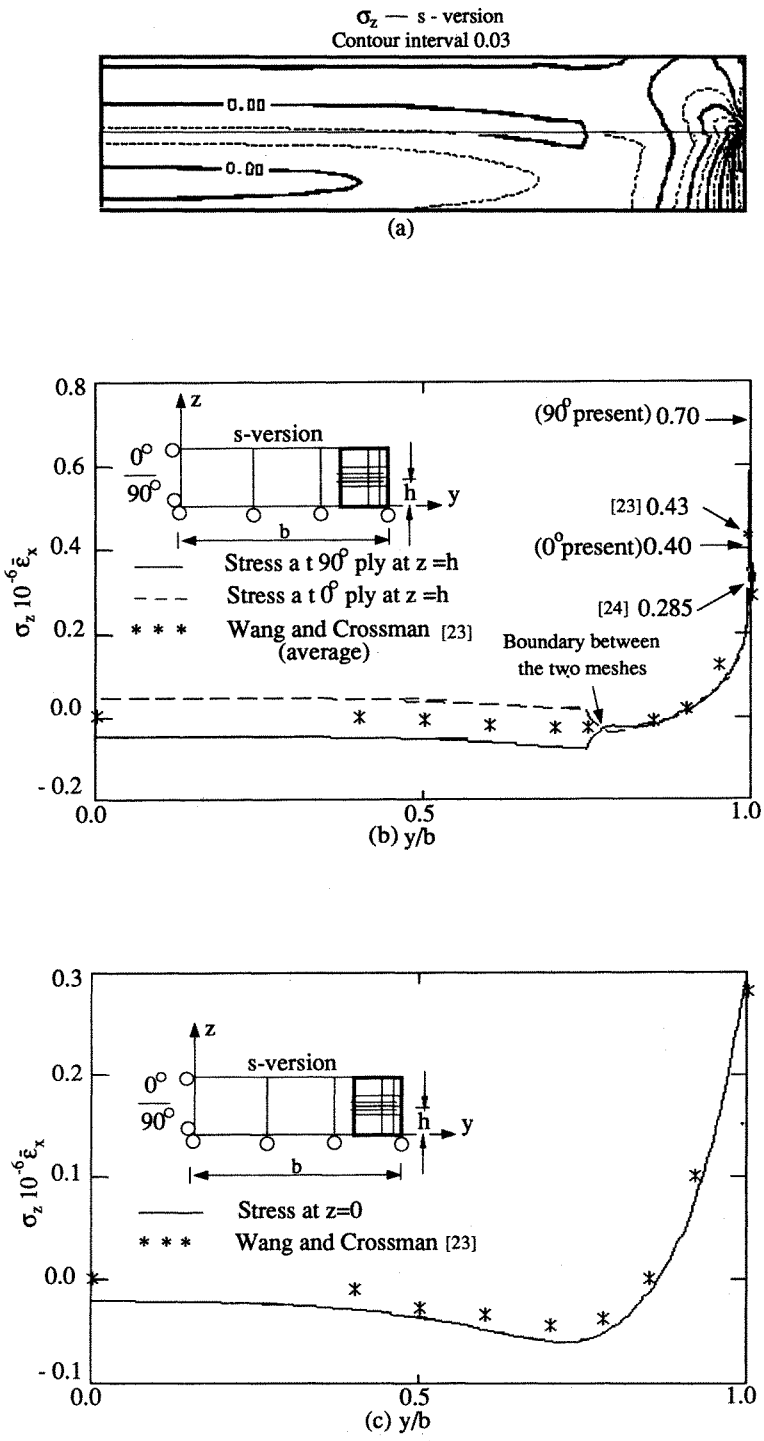

Figure 18. Contour plots and distribution of σ_z along $z = 0$ and $z = h$ in axial tension problem as obtained with s-method

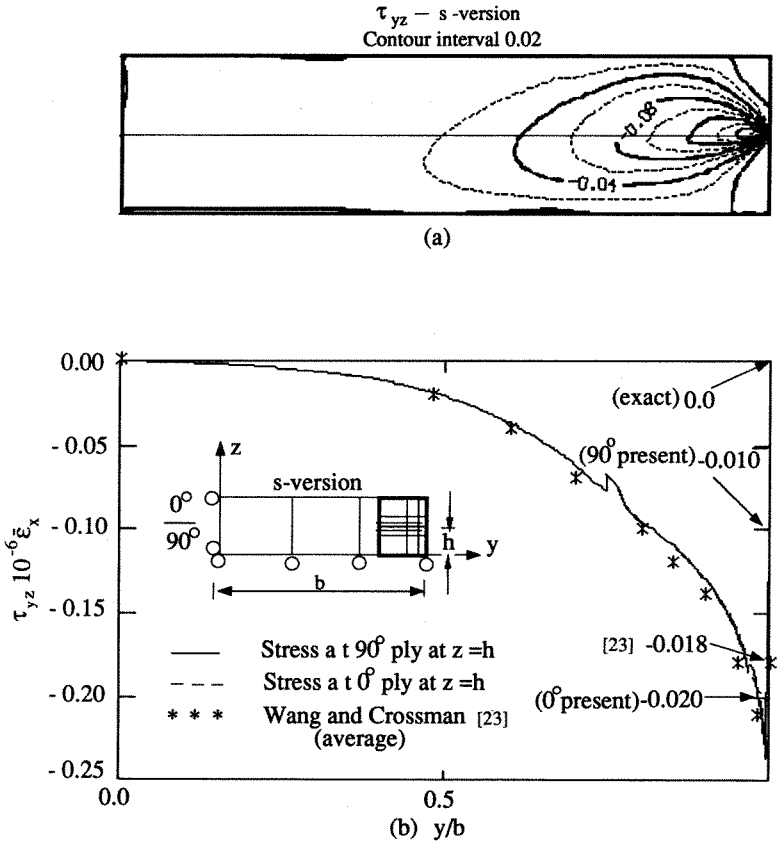

Figure 19. Contour plots and distribution of τ_{yz} along $z = h$ in axial tension problem as obtained with *s*-method

ACKNOWLEDGEMENT

The support of the National Science Foundation under Research Initiation Award ECS–9003093 is gratefully acknowledged.

REFERENCES

1. C. T. Achenbach, C. T. Sun and G. Herrmann, 'Continuum theory for a laminated body', *J. Appl. Mech. ASME*, **35,** 467 (1968).
2. R. L. Spilker, 'A hybrid-stress finite-element formulation for thick multilayer laminates', *Comp. Struct.*, **11,** 507–514 (1980).
3. E. Reissner and Stavsky, 'Bending and stretching of certain types of heterogeneous aeolotropic elastic plates', *J. Appl. Mech. ASME*, **28,** 402 (1961).
4. J. M. Whithey and N. J. Pagano, 'Shear deformation in heterogeneous plates', *J. Appl. Mech. ASME*, **27,** 1031 (1970).
5. J. M. Whitney and C. T. Sun, 'A higher order theory for extensional motion of laminated composites', *J. Sound Vib.*, **30,** 85–97 (1973).
6. R. B. Nelson and D. R. Lorch, 'A refined theory of laminated orthotropic plates', *J. Appl. Mech. ASME*, **41,** 177–183 (1974).
7. K. H. Lo, R. M. Christensen and E. M. Wu, 'A higher-order theory of plate deformation, Part 2: Laminated plates', *J. Appl. Mech. ASME*, **44,** 669–676 (1977).
8. M. Levinson, 'An accurate simple theory of the statics and dynamics of elastic plates', *Mech. Res. Commun.*, **7,** 343–350 (1980).

9. J. N. Reddy, 'A simple higher-order theory for laminated composite plates', *J. Appl. Mech. ASME*, **51,** 745–751 (1984).
10. R. L. Spilker and D. M. Jacobs, 'Hybrid stress reduced-Mindlin elements for thin multilayer plates', *Int. j. numer. methods eng.*, **23,** 555–578 (1986).
11. S. Tang, 'A boundary layer theory—Part 1: laminated composites in plane stress', *J. Compos. Mater.*, **9,** 33–41 (1975).
12. B. N. Pandya and T. Kant, 'Higher-order shear deformable theories for flexure of sandwich plates—finite element evaluation', *Int. J. Solids Struct.*, **24,** 1267–1286 (1988).
13. D. Engrand, 'Local effects calculations in composite plates by boundary layer method', in P. Ladeveze (ed.), *Local Effects in the Analysis of Structures*, Elsevier, New York, 1985.
14. C. D. Mote, 'Global–local finite element', *Int. j. numer. methods eng.*, **3,** 565–574 (1971).
15. R. I. Zwiers, T. C. T. Ting and R. L. Spilker, 'On the logarithmic singularity of free-edge stress in laminated composites under uniform extension', *J. Appl. Mech. ASME*, **49,** 561–569 (1982).
16. A. K. Noor, 'Global–local methodologies and their application to nonlinear analysis', *Finite Elements Anal. Des.*, **2,** 333–346 (1986).
17. J. Fish, 'The *s*-version of the finite element method', *Comp. Struct.*, to appear.
18. N. J. Pagano and S. R. Soni, 'Global–local laminate variational model', *Int. J. Solids Struct.*, **19,** 207–228 (1983).
19 A. G. Peano, 'Hierarchies of conforming finite elements for plane elasticity and plate bending', *Comp. Math. Appl.*, **2** (1976). pp. 211–224.
20. O. C. Zienkiewicz and K. Morgan, *Finite Elements and Approximations*, Wiley, New York, 1983.
21. T. Belytschko, J. Fish and A. Bayliss, 'The spectral overlay on the finite element solutions with high gradients', *Comp. Methods Appl. Mech. Eng.*, **81,** 71–89 (1990).
22. N. J. Pagano, 'Exact solutions for composite laminates in cylindrical bending', *J. Compos. Mater.*, **3,** 398–411 (1969).
23. A. S. D. Wang and F. W. Crossman, 'Some new results on edge effects in symmetric composite laminates', *J. Compos. Mater.*, **8,** 65 (1974).
24. R. L. Spilker, 'Edge effects in symmetric composite laminates: importance of satisfying the traction-free-edge condition', *J. Compos. Mater.*, **14,** 2–20 (1980).
25. B. A. Szabo, 'Esitmation and control of error based on *p* convergence', in I. Babuska *et al.* (eds.), *Accuracy Estimates and Adaptive Refinements in Finite Element Calculations*, Wiley, New York, 1986, pp. 61–79.
26. B. A. Szabo and G. J. Sharman, 'Hierarchic plate and shell models based on *p*-extension', *Int. j. numer. methods eng.*, **26,** 1855–1881 (1988).